



Mass-shift mode to quantify low level ^{129}I in environmental samples by ICP-MS/MS

Coralie Carrier, Azza Habibi, Michelle Agarande, Celine Augeray, Didier Bourlès, Denis Maro, Lucilla Benedetti

► To cite this version:

Coralie Carrier, Azza Habibi, Michelle Agarande, Celine Augeray, Didier Bourlès, et al.. Mass-shift mode to quantify low level ^{129}I in environmental samples by ICP-MS/MS. *Journal of Analytical Atomic Spectrometry*, 2022, 37 (6), pp.1309-1317. 10.1039/D2JA00128D . hal-03704429

HAL Id: hal-03704429

<https://hal.science/hal-03704429>

Submitted on 24 Jun 2022

HAL is a multi-disciplinary open access archive for the deposit and dissemination of scientific research documents, whether they are published or not. The documents may come from teaching and research institutions in France or abroad, or from public or private research centers.

L'archive ouverte pluridisciplinaire **HAL**, est destinée au dépôt et à la diffusion de documents scientifiques de niveau recherche, publiés ou non, émanant des établissements d'enseignement et de recherche français ou étrangers, des laboratoires publics ou privés.

Mass-shift mode to quantify low level ^{129}I in environmental samples by ICP-MS/MS

CARRIER Coralie^a, HABIBI Azza^a *, AGARANDE Michelle^a, AUGERAY Celine^a, BOURLES Didier^{b†}, MARO Denis^c, BENEDETTI Lucilla^b

^aInstitut de Radioprotection et de Sûreté Nucléaire, PSE-ENV/SAME/LERCA, 31 rue de l'écluse, 78116 Le Vésinet, France.

*Email : azza.habibi@irsn.fr

^bAix Marseille Univ, CNRS, Centrale Marseille, M2P2, Technopôle de l'Arbois, 13545 Aix en Provence, France

^cInstitut de Radioprotection et de Sûreté Nucléaire, PSE-ENV/SRTE/LRC, Rue Max Pol Fouchet, 50130 Cherbourg-Octeville, France

† This article is dedicated to Didier Bourlès

Abstract

In this study, a new measurement method to quantify ^{129}I at low level by ICP-MS/MS (Agilent 8900) was developed. This new method is based on a new measurement medium and mass-shift mode. The developed measurement medium is composed of 0.1% NH_4OH , 10 g L^{-1} ascorbic acid and 3% Tween® 20 which considerably decrease the memory effect and increase the sensitivity. Different reactional gas were compared on on-mass and mass-shift modes and finally, O_2 was selected on mass-shift mode. The mass-shift mode with O_2 allows having the most quantitative iodine oxidation rate while eliminating isobaric and polyatomic interferences. Isobaric interference due to $^{129}\text{Xe}^+$ is eliminated following a charge transfer in the reaction/collision cell and polyatomic interferences are eliminated with the second quadrupole. This new measurement method improves the limit of detection of ^{129}I to 11 mBq L^{-1} , without chemical treatment.

Introduction

Iodine is an extremely volatile halogen (it sublimates at room temperature) naturally occurring under various organic or inorganic forms e.g. CH_3I , I_2 , I^- , IO_3^- , CH_2I_2 ... This element can exist in the environment with different oxidation states¹ : -I, 0, +I, +V and +VII. These physico-chemical characteristics complicate its reliable quantification. Among the 37 iodine isotopes, ^{127}I is the only stable one and ^{129}I is the naturally occurring radioactive isotope with the longest half-life (16.1×10^6 y)².

^{129}I is a beta, X and gamma emitter, it is therefore often measured by gamma or X-ray spectrometry^{3–5}. Gamma and X-rays emission energies and intensities are however low (e.g. 39.6 KeV (7.5%) for gamma ray and 29.5 KeV (20.4%) and 29.8 KeV (37.7%) for X-rays. These properties induce high limits of detection (0.1 – 0.2 Bq L^{-1}). As a consequence, the isotopic ratio $^{129}\text{I}/^{127}\text{I}$, which is useful for dating or tracing purposes but is very low in environmental samples, is below the detection limit with radiometric technics.

Indeed, in environmental samples, the natural isotopic ratio $^{129}\text{I}/^{127}\text{I}$ is near 10^{-11} and can reach 10^{-3} close to Nuclear Fuel Reprocessing Plant (NFRP); e.g. La Hague (France) and Sellafield (UK). To be able to accurately measure all the range of this isotopic ratio, a lower ^{129}I limit of detection is needed^{6,7}.

To improve the limit of detection and quantify the isotopic ratio, neutron activation analysis (NAA) has been used by converting ^{129}I to **short-lived** ^{131}I which is measured by gamma spectrometry. The work published by Fan *et al.* allows reaching a limit of detection for 10^{-10} for $^{129}\text{I}/^{127}\text{I}$ after an appropriate chemical treatment⁸.

Accelerator Mass Spectroscopy (AMS) is a very efficient technique to measure iodine 129 and $^{129}\text{I}/^{127}\text{I}$ and has been the subject of various studies^{9,10}. In fact, AMS allows reaching low limits of detection^{11,12} (e.g. 0.05 $\mu\text{Bq L}^{-1}$ and 10^{-14} for ^{129}I and $^{129}\text{I}/^{127}\text{I}$, respectively). However, due to the acquisition and functioning costs, there are only 110 AMS in the world and according to Kutschera¹³, only 22 allow ^{129}I measurement.

Several recent works have shown that ICP-MS (Inductively Coupled Plasma – Mass Spectrometry) and more specifically ICP-MS/MS is an excellent and affordable alternative to AMS for the measurement quantification of ^{129}I and the isotopic ratio $^{129}\text{I}/^{127}\text{I}$ ^{7,14,15} with a limit of detection of ~ 100 mBq L^{-1} and 10^{-6} , respectively, without chemical treatment. This quantification is however a real challenge due to the extreme volatility of iodine which could decrease sensitivity and induce memory effects. To minimize iodine volatility, the analysis medium by ICP-MS is often NH_4OH or TMAH^{16,17}.

The major interference at m/z 129 is due to the isobar $^{129}\text{Xe}^+$ which is present as impurity in the plasma Ar gas.

$^{129}\text{I}^+$ has also polyatomic interferences e.g. $^{89}\text{Y}^{40}\text{Ar}^+$, $^{115}\text{In}^{14}\text{N}^+$, $^{113}\text{InO}^+$, $^{113}\text{Cd}^{16}\text{O}^+$, $^{97}\text{Mo}^{16}\text{O}_2^+$, $^{127}\text{IH}_2^+$ and $^{127}\text{ID}^+$ ^{18–20}.

The aim of this work is to present a new methodology allowing to decrease the limit of detection of ^{129}I and then of the isotopic ratio $^{129}\text{I}/^{127}\text{I}$ when the measurement is performed by ICP-MS/MS.

Experimental

Reagents

Ascorbic acid, oxalic acid, hydroxylammonium chloride and NaI solutions are prepared from analytical-grade powder provided by VWR chemicals. Potassium iodate and iodide for laboratory use are from Chem-lab analytical. Analytical grade 20% (v/v) NH_4OH and biology grade Triton® X-100 are from BDH Prolabo®. 25% (v/v) tetramethylammonium hydroxide (TMAH) electronic grade is provided by Alfa Aesar.

Tween® 20, Tween® 80, Tergitol™ and Brij™ C20 are from fisher scientific, Acros Organics™.

Mono-elemental solution (e.g. Mo, In, Cd, Y and Te) are obtained from SCP science and certificated to be at $995 \pm 4 \mu\text{g ml}^{-1}$; $1000 \pm 4 \mu\text{g ml}^{-1}$; $1004 \pm 6 \mu\text{g ml}^{-1}$; $1004 \pm 4 \mu\text{g ml}^{-1}$ and $996 \pm 6 \mu\text{g L}^{-1}$ respectively.

All dilutions are done with ultrapure water ($18.2 \Omega\text{M cm}$, Merck Millipore).

For this study, two certificated ^{129}I standard, I129ELSB30 and I129ELSB200KBQ, are supplied by ORANO LEA (Tricastin, France).

He, N_2O , O_2 and CO_2 analytical grade gases are from Air Products.

Water samples

For the method development, water solutions containing $0.01 \mu\text{g L}^{-1}$ to $100 \mu\text{g L}^{-1}$ of NaI were prepared.

To verify the accuracy of the method, Milli-Q water (for synthetic samples) and natural river water samples collected in France, not originally containing any ^{129}I detectable traces, were spiked with I129ELSB30 ^{129}I standard. Water samples were previously filtered with $0.45 \mu\text{m}$ syringe filter. The final activity concentration ranged from 0.02 Bq L^{-1} to 10 Bq L^{-1} .

Instrument

^{129}I and ^{127}I are measured using the Agilent 8900 ICP-QQQ in MS/MS mode (Agilent Technologies, Tokyo, Japan). The experimental parameters are listed in table 1.

Table 1 - Experimental parameters of the ICP-MS/MS

RF power	1520 W
RF matching	2.30 V
Sampling depth	5.3 mm
Nebulizer gas flow rate	1.05 L min^{-1}
Solution uptake rate	1.2 mL min^{-1}
Spray chamber temperature	0°C
Extraction lens 1; 2	-29.3 V; -205.5 V
Deflect	8 to 13 V
Energy discrimination	-8 to -4 V
Axial acceleration	0 V
Plate bias	-110 to -50 V
Octupole bias	-25 to -20 V
Cell entrance	-75 to -5 V
Cell exit	-135 to -120 V

For all batches, monitored m/z are 126, 127, 129, 130, 142, 143, 145 and 146. For each sample injection, 5 replicates are done, with 300 sweeps replicates with 1 point per peak. Daily tuning is realized with a ^{127}I $100 \mu\text{g L}^{-1}$ solution. Energy discrimination, defect and plate bias has the most important effect on the sensitivity.

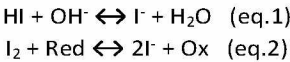
When MS/MS mode is used, octopole bias, cell entrance and cell exit are the most impactor parameters on sensitivity. O_2 , CO_2 and N_2O gas were introduced through the 4th gas inlet line.

Rinsing solution after each sample is 0.1% (v/v) NH_4OH .

Results and discussion

Measurement medium

Due to its extreme volatility and its complex redox properties, the nature of iodine measurement medium is essential. Indeed, in alkaline and reducing media and according to equations (1) and (2), formation of volatile iodine species (e.g. I₂ and HI) is avoided and iodide species is predominant.



Red = Reducing agent; Ox = Oxidizing agent

In environmental water samples, iodide and iodate could be present ²¹. Fig.1 shows ICP-MS signal intensity variation during single quadrupole measurement of iodine solution at 100 μg L⁻¹ prepared with KI and KIO₃ in NH₄OH at different pH.

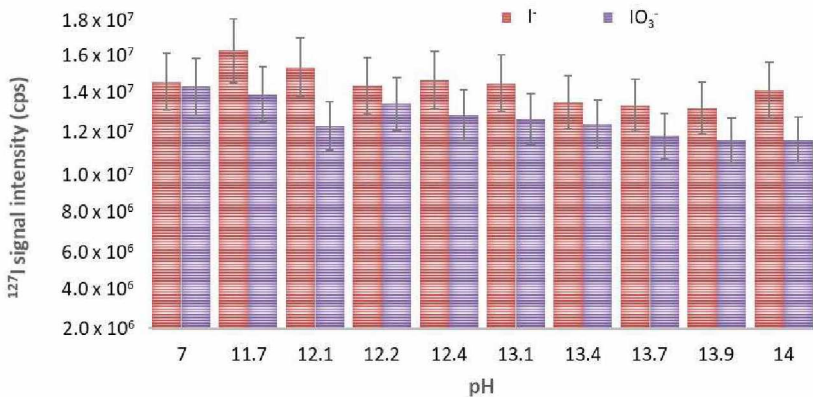


Fig. 1 ICP-MS signal intensity (cps) variation for 100 μg L⁻¹ of ¹²⁷I in NH₄OH solutions ranging from pH 7 to 14. On-mass measurement mode. Error bars are estimated at 10%.

Obtained results show that ¹²⁷I signal intensity variation is within the error bars regardless of the pH and the iodine form (I⁻ or IO₃⁻) (Fig.1). 0.1% NH₄OH (pH = 12) is selected for practical preparation reasons for the following tests and for rinses between samples.

The memory effect is very impacting when analysing iodine by ICP-MS. This disadvantage is due to the extreme volatility of iodine that accumulates and adsorbs on the ICP-MS introduction system. To minimize this impact during ICP-MS iodine measurement, the use of a non-ionic surfactant could be efficient since it allows avoiding losses due to adsorption to the introduction system of the ICP-MS.

Fig.2 presents the variation of signal intensity of ¹²⁷I when measuring 100 μg L⁻¹ of ¹²⁷I in 0.1% (v/v) NH₄OH containing different non-ionic surfactants e.g. Tergitol™ 15-S-9, Triton® X-100, Brij™ C20, Tween® 20 and Tween® 80, with concentrations ranging from 0.5% (v/v) to 3% (v/v). The viscosity of these surfactants make it difficult to handle concentrations higher than 3%. ²²⁻²⁴.

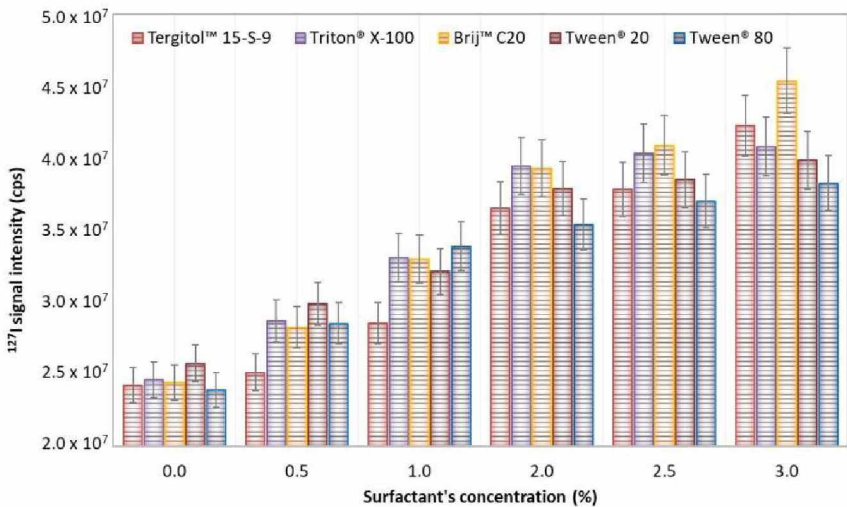


Fig. 2 - ¹²⁷I 100 μg L⁻¹ ICP-MS signal intensity (cps) in 0.1% (v/v) NH₄OH using different surfactants: Tergitol™ 15-S-9, Triton® X-100, Brij™ C20, Tween® 20 and Tween® 80. On-mass measurement mode. Error bars represent 10%.

Results presented in fig.2 show that ^{127}I signal intensity is proportional to surfactants concentration. A content of 3% is then retained since it allows a signal gain of 2.5. The ICP-MS sensitivity gap is within the error bars regardless of the surfactant.

Tween™ 20 is not hazardous and less viscous than the others with the lowest CMC (Critical Micelle Concentration) of 60 ppm. This surfactant is then used for the rest of the study.

Moreover, a reducing agent can prevent iodine's oxidization and the formation of I_2 (eq. 2). Four reducing agents with standard potentials below that of the couple I_2/I^- (0.54 V) were then compared^{25–27}: ascorbic acid (0.13 V), oxalic acid (–0.47 V), sodium sulphide (–0.93 V) and hydroxylammonium chloride (–1.05 V). Solutions of 0.1% (v/v) of NH_4OH containing 3% (v/v) of Tween 20, $100\ \mu\text{g L}^{-1}$ of NaI and a reducing agent were prepared. In order to prevent the ICP-MS introduction system clogging, reducing agents concentrations did not exceed $10\ \text{g L}^{-1}$. These solutions were also compared to TMAH 1% (v/v), often used as measurement media to analyse iodine by ICP-MS^{19,28,29}. In order to evaluate the memory effect, measurements are followed by four 0.1% (v/v) NH_4OH rinses with a duration of 5 min each (fig.3). ^{127}I signal is monitored after each rinse.

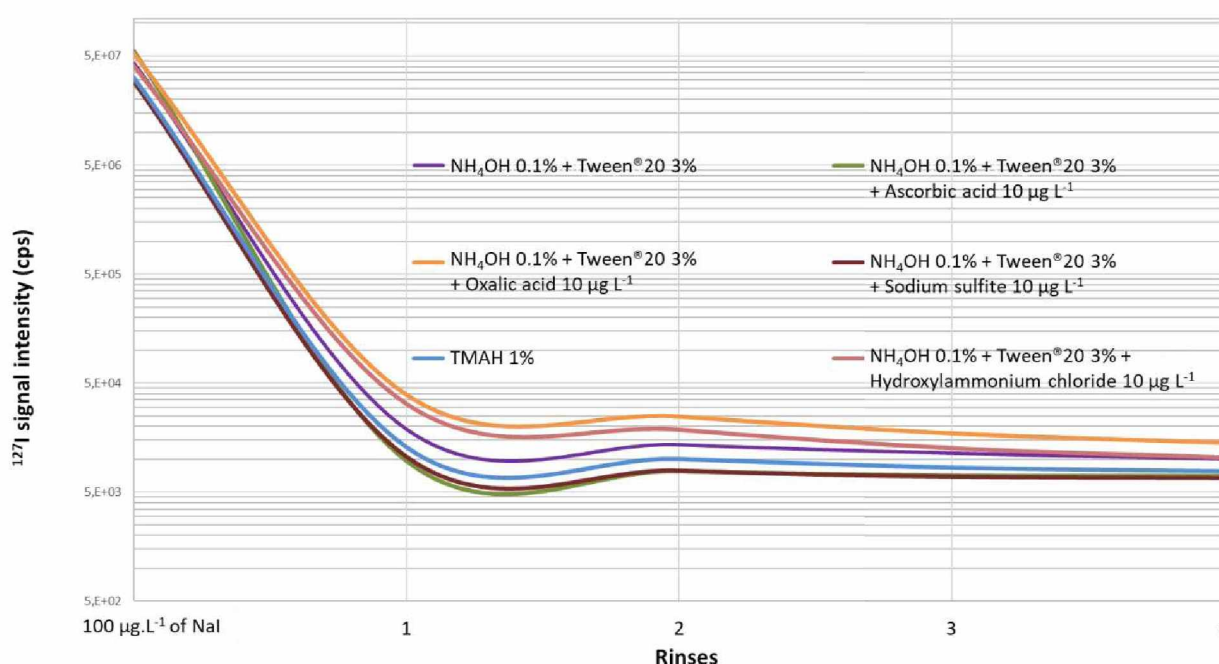


Fig. 3 - ^{127}I signal evolution when using reducing agents with tween® 20 or TMAH – On-mass measurement mode.

Memory effect is clearly visible in fig.3. After introduction of $100\ \mu\text{g L}^{-1}$ of NaI , the residual signal could reach 35000 cps and would have a significant impact on quantification. It decreases with 0.1% (v/v) NH_4OH rinses. The addition of a reducing agent to the measurement medium reduces the memory effect. According to results presented in fig. 3, the most efficient reducing agent is ascorbic acid with a concentration of $10\ \text{g L}^{-1}$ since it minimizes the memory effect to only 0.15% of the initial signal.

The various tests carried out in this study and illustrated in Fig. 1, 2 and 3 permitted to select an optimal measurement medium (OM) composed of 0.1% of NH_4OH (v/v), 3% (v/v) of Tween 20 and $10\ \text{g L}^{-1}$ of ascorbic acid. This measurement medium allows minimizing memory and matrix effect which increase the sensitivity. It was compared to TMAH 1% (v/v) and 2% (v/v), (fig.4).

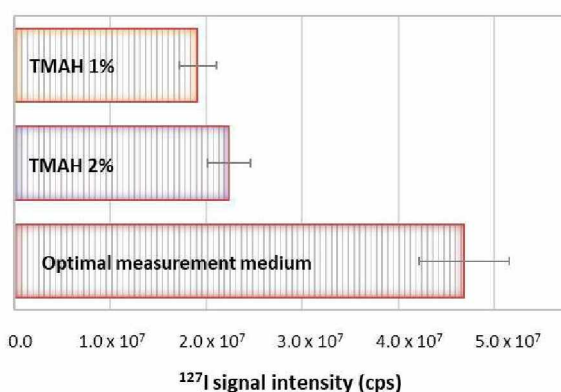


Fig. 4 - ICP-MS signal intensity at m/z 127 for 100 µg L⁻¹ in TMAH and in the optimal medium. On-mass measurement mode. Error bar represents 10%.

According to results presented in the fig. 4, the signal obtained at m/z 127 when analysing 100 µg. L⁻¹ of NaI in the newly developed medium is more than 2 times higher than the signal obtained when iodine is in 2% (v/v) TMAH. Signal intensity at m/z 129 in blanks of these 3 media were then compared at m/z 129 for TMAH 1%, TMAH 2% and OM respectively.

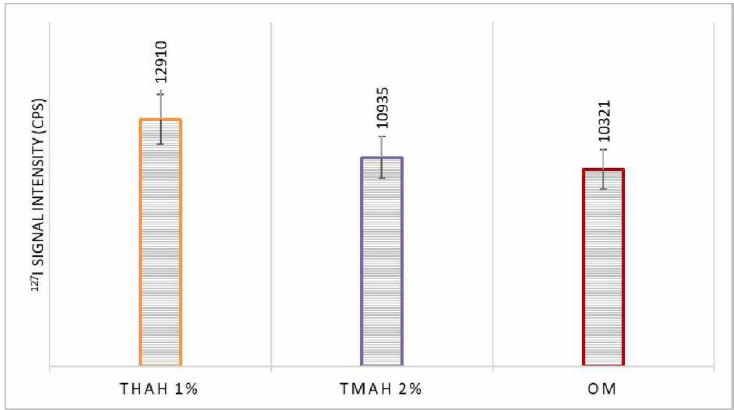
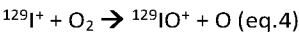
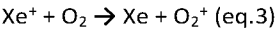


Figure 5 - Signal intensity at m/z 129 for Blanks of 3 media. On-mass measurement mode. Error bar represents 10%.

According to fig. 5, signal intensity for these 3 media at m/z 129 is the same within the error bars. These results permit to confirm the efficiency of the newly developed measurement medium since the signal/noise is the highest.

¹²⁹Xe⁺ isobaric interference

¹²⁹Xe⁺, the major ¹²⁹I⁺ interference is present as an impurity in the argon gas. Its removal is then not possible with a chemical treatment prior to measurement. ¹²⁹Xe⁺ content is variable from one gas tank to another and xenon abundance shows a bias with the natural expected value. An accurate afterward correction by calculation is then complicated. In order to eliminate this interference, all published works use oxygen with flow rates between 20% and 60% in on-mass mode to perform a charge transfer as shown in fig. 6 (eq.3).



In these conditions, signal due to ¹²⁹Xe⁺ is greatly reduced^{19,20,29} but not completely eliminated. Furthermore, although iodine oxidation by O₂ (eq. 4) is not thermodynamically favourable ($\Delta H_r = 2.08 \text{ eV}$)¹⁵, this chemical reaction takes place inside the collision/reaction cell (fig. 6) and therefore directly affect the sensitivity of iodine. The fraction of iodine that is oxidized in these conditions has never been reported.

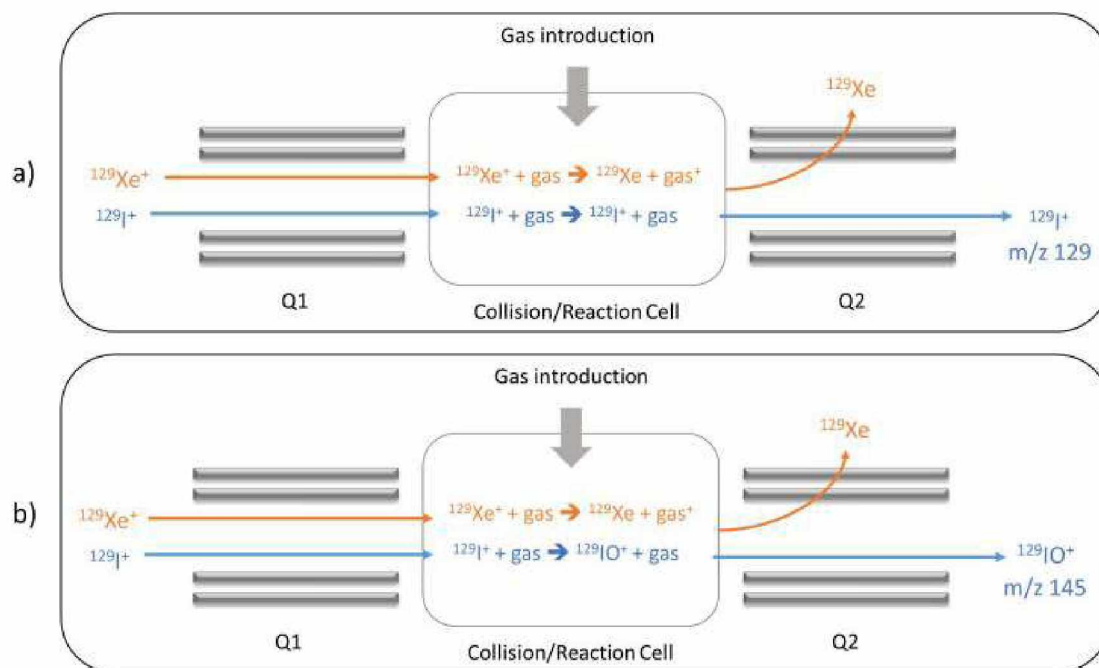


Fig. 6– a) On-mass mode for ^{129}I determination with $^{129}\text{Xe}^+$ interference elimination by charge transfer
b) Mass-shift mode for ^{129}I determination with oxidizing gas

In order to improve iodine limit of detection and obtain the highest signal/noise (S/N), oxidized iodine fraction has to be minimized in on-mass mode by using a less oxidizing gas such as CO_2 . In fact, according to Tanner *et al.*, CO_2 is a less oxidizing gas than O_2 since its O-atom affinity is stronger³⁰. The use of CO_2 to quantify iodine in on-mass mode is then supposed to improve iodine detection recovery while reducing xenon signal following a charge transfer in the collision/reaction cell.

In this study, iodine detection in mass-shift mode was also investigated in order to improve the limit of detection. Besides O_2 , a more oxidizing gas e.g. N_2O was then used³⁰. This alternative could allow decreasing the limit of detection since ^{129}I will be detected at m/z 145 ($^{129}\text{I}^{16}\text{O}^+$). At m/z 145, signal due to $^{129}\text{Xe}^+$ will be negligible since the oxidation of xenon is not favourable.

Solutions containing $100 \mu\text{g. L}^{-1}$ of stable iodine in OM were measured by ICP-MS/MS in on mass and mass-shift modes, using several gases (O_2 , N_2O and CO_2) at different flow rates (0% to 30%) and with two different nebulizers (e.g. MicroFlow inert PFA and glass concentric nebulizers). Obtained signal at m/z 143 ($^{127}\text{I}^{16}\text{O}^+$) are presented in fig.7.

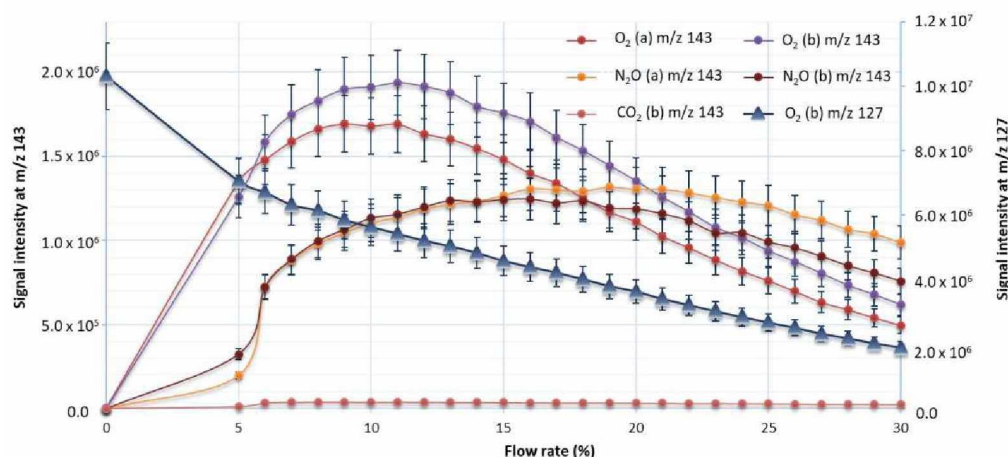


Fig. 7 – Signal intensity at m/z 127 on on-mass mode and m/z 143 on mass-shift mode with O_2 , N_2O and CO_2 in OM for $100 \mu\text{g L}^{-1}$ of ^{127}I solution: (a) MicroMist micro-uptake glass concentric nebulizer and (b) MicroFlow inert PFA. Error bars represent 10%.

Results show that over 15% of initially detected iodine 127 is oxidized at O₂ flow rate of 8% comparing to oxygen free measurements. Counts at m/z 145 induced by xenon were also monitored and, as expected, the signal was less than 20. To improve the sensitivity, a MicroFlow inert PFA was used and allowed a sensitivity gain of approximately 10% (fig.7). The signal stability is extremely satisfactory with an RSD always lower than 5%.

APEX-Q introduction system, a desolvating module was considered to improve the sensitivity. However, the principle of this module based on the heat of the sample, is not compatible with physicochemical characteristics of iodine (e.g. extreme volatility)³¹.

As expected, fig.7 shows that iodine is less oxidized with CO₂ than with O₂. The sensitivity is however similar when using a MicroFlow inert PFA nebulizer or a MicroMist micro-uptake glass concentric nebulizer. Using CO₂ could be an alternative to avoid iodine's oxidation and then improve the limit of detection when the measurement is performed in on-mass mode.

Despite N₂O being a more oxidizing gas than O₂³⁰, counts at m/z 143 when using this gas are lower than those obtained with O₂ probably due to the size of N₂O and to the loss of a fraction of iodine by collision.

To improve ions focalization, helium gas was used with concentrations between 0.5% and 10%. Obtained results with and without addition of He are similar. The following tests were then carried out without addition of helium.

To determine the best mode and gas combination, limits of detection were calculated for flows providing the highest signal/noise and presented in fig.8.

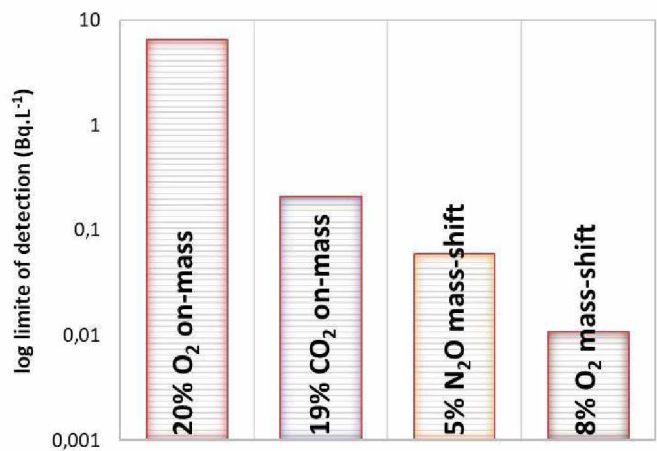


Fig. 8 - Obtained limits of detection with different gas and modes with a microFlow inert PFA nebulizer in OM.

According to figure 8, the lower limit of detection (LOD) for iodine 129 is obtained with mass-shift mode with oxygen and a PFA nebulizer. This configuration allows having the best signal/noise ratio (S/N). Moreover, since only 15% of ¹²⁷I on mass-shift mode are detected, concentration that can be measured before the detector saturation are higher than on on-mass mode. Consequently, the obtained ¹²⁹I/¹²⁷I could be lower than that obtained on on-mass mode by several orders of magnitude. To obtain the best limit of detection, integration time was optimized to 1 s and LOD was then estimated to 11 mBq.L⁻¹ without chemical treatment. The limit of quantification (LOQ) of ¹²⁹I was estimated to 25 mBq L⁻¹.

Polyatomic interference of IOH₂⁺ and IOD⁺ and abundance sensitivity

Polyatomic interferences³² at m/z 145 due to ¹²⁷I¹⁶O¹H₂⁺ and ¹²⁷I¹⁶O²D⁺ could be formed during the measurement process in mass-shift mode. To evaluate this interference, solutions ranging from 1 µg L⁻¹ to 1 g L⁻¹ of ¹²⁷I were prepared in OM and measured by ICP-MS.

Table 2 - ¹²⁷I¹⁶O¹H₂⁺ and ¹²⁷I¹⁶O²D⁺ influence at m/z 145 in mass-shift mode

¹²⁷ I Concentration (mg L ⁻¹)	CPS at m/z 143	CPS at m/z 145
10 ⁻³	21513	62
10 ⁻²	211480	56
10 ⁻¹	2262501	51
1	17575881	50
10	184781576	81
10 ²	1524546033	296

0.5×10^3	5934641511	489
10^3	9988338422	617

Mass-shift ICP-MS/MS measurement of these solutions highlighted that for ^{127}I concentrations $< 10 \text{ mg L}^{-1}$, counts at m/z 145 are near the background.

However, when concentration are $> 10 \text{ mg L}^{-1}$, $^{127}\text{I}^{16}\text{O}^{16}\text{H}_2^+$ and $^{127}\text{I}^{16}\text{O}^{16}\text{D}^+$ interferences and the abundance sensitivity are clearly observable. This concentration is higher than that observed in environmental samples.

For an accurate determination of $^{129}\text{I}/^{127}\text{I}$, the contribution of ^{127}I at m/z 145 is corrected by measuring a solution containing ^{127}I and using the ratio $^{127}\text{IOH}_2^+/^{127}\text{IO}^+$.

Other polyatomic interferences

The other polyatomic interferences at m/z 129 are due to $^{89}\text{Y}^{40}\text{Ar}^+$, $^{115}\text{In}^{14}\text{N}^+$, $^{113}\text{InO}^+$, $^{113}\text{Cd}^{16}\text{O}^+$, $^{97}\text{Mo}^{16}\text{O}_2^+$, $^{127}\text{IH}_2^+$ and $^{127}\text{ID}^+$.

In the environment, yttrium, molybdenum, indium and cadmium are present at concentrations ranging from 1 ng L^{-1} to 200 mg L^{-1} ^{33–35}. When ^{129}I measurement is performed by ICP-MS/MS in mass-shift mode, the first filter is set at m/z 129 and the second filter is set at m/z 145. This configuration is more consistent than on-mass mode measurement since it allows the elimination of the polyatomic interferences according to fig.9.

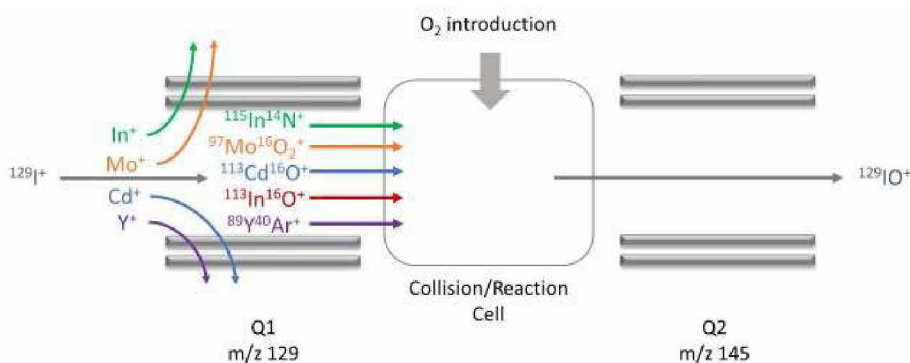


Fig. 9 - Interferences behaviour for Q1 \rightarrow m/z 129 and Q2 \rightarrow m/z 145 with O_2 in the collision/reaction cell and detection on mass-shift measurement mode.

This statement was experimentally verified by measuring solutions containing $1 \mu\text{g L}^{-1}$ to 100 mg L^{-1} of interferences on mass-shift mode with oxygen. Monitored m/z were 105, 113, 129, 131 and 145.

As expected, none of these elements disturb the ^{129}I measurement in mass-shift mode since no signal is detected above the background at m/z 145.

Quantification of ^{127}I

In this study, ^{129}I quantification in environmental samples is based on the isotopic dilution method where ^{127}I will be used as internal standard. In order to do this, ^{127}I has to be previously quantified.

In literature, ^{127}I is often quantified using external calibration corrected by Sb, Te, Re or Cs as internal standard^{17,36,37}. We chose to use ^{126}Te because its m/z and ionization energy (9.01 eV) are close to iodine's (10.45 eV). The linearity of the pulse and analogue detection is demonstrated by measuring standards up to 1 mg L^{-1} and having correlation coefficient higher than 0.999 for several calibration curves.

^{127}I limits of detection and quantification in mass-shift mode when monitored m/z are 142 ($^{126}\text{Te}^{16}\text{O}^+$) and 143 ($^{127}\text{I}^{16}\text{O}^+$) were estimated to be $0.15 \mu\text{g L}^{-1}$ and $0.4 \mu\text{g L}^{-1}$ respectively.

To verify the accuracy of the ^{127}I quantification method, several solutions were prepared in water with different concentrations. Three different tests were realized with I^- , IO_3^- and a mix of $\text{I}^- + \text{IO}_3^-$ (50/50) in the newly developed

medium. Expected and measured concentrations are then compared. Table 3 shows calculated Bias (eq. 7) and standardized deviation (SD) (eq. 8).

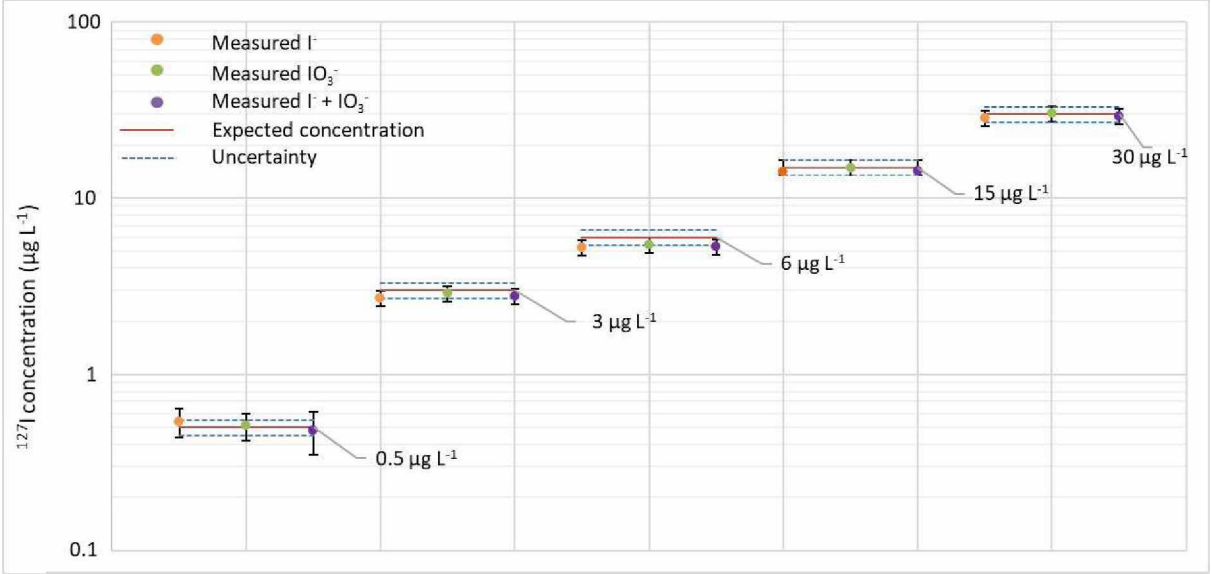


Figure 10 - ¹²⁷I quantification in synthetic samples in mass-shift mode in OM. Error bars represents calculated uncertainties

According to results presented in Fig. 10, measured concentrations are in good agreement with the expected values whether iodine is under I⁻ or IO₃⁻ form for a large range of concentrations.

Quantification of ¹²⁹I

In order to confirm the applicability of the method, synthetic solutions and river water samples free from ¹²⁹I are spiked with ¹²⁷I and ¹²⁹I which are quantified following the procedure described above. The obtained results are presented in table 2.

$$\text{Bias (\%)} = \left| \frac{[^{127}\text{I}]_{\text{mes}} - [^{127}\text{I}]_{\text{th}}}{[^{127}\text{I}]_{\text{th}}} \right| \times 100 \quad (7)$$

$$\text{SD} = \frac{|[^{127}\text{I}]_{\text{mes}} - [^{127}\text{I}]_{\text{th}}|}{\sqrt{U^2[^{127}\text{I}]_{\text{mes}} + U^2[^{127}\text{I}]_{\text{th}}}} \quad (8)$$

[¹²⁷I]_{th} = Expected ¹²⁷I concentration (µg L⁻¹)
[¹²⁷I]_{mes} = Mesured ¹²⁷I concentration (µg L⁻¹)
U²[¹²⁷I]_{th} = Uncertainty associated to theoretical ¹²⁷I concentration
U²[¹²⁷I]_{mes} = Uncertainty associated to measured ¹²⁷I concentration

Table 2 - ¹²⁹I quantification in spiked synthetic and river water samples

Sample	Theoretical activity (Bq L ⁻¹); k=2	Measured activity (Bq L ⁻¹); k=2	Bias (%)	SD
River water (1)	0.020 ± 0.002	0.022 ± 0.019	10	0.002
	0.070 ± 0.007	0.070 ± 0.014	< 1	< 0.001
	0.200 ± 0.020	0.220 ± 0.020	10	0.021
	0.500 ± 0.050	0.476 ± 0.015	5	0.025
River water (2)	0.020 ± 0.002	0.020 ± 0.019	< 1	< 0.001
	0.080 ± 0.008	0.072 ± 0.053	10	0.005
Synthetic samples	0.200 ± 0.020	0.208 ± 0.020	4	0.008
	0.500 ± 0.050	0.564 ± 0.015	13	0.065

	1.000 ± 0.100	1.013 ± 0.040	1	0.009
	10.000 ± 1.000	10.457 ± 0.020	5	0.167

According to results obtained when analyzing synthetic and natural river water samples, measured activities are in perfect agreement with the expected activities. These good performances are characterized by bias (eq.7) lower than 15% and standardized deviation (eq.8) lower than 2 even for activities close to ^{129}I LOQ (25 mBq L⁻¹).

Isotopic ratio determination

Spiked water samples with $^{129}\text{I}/^{127}\text{I}$ ratios ranging from 3.0×10^{-8} to 3.8×10^{-9} were prepared from I129ELSB200KBQ (Orano Lea) and analyzed using the newly developed method. This determination of $^{129}\text{I}/^{127}\text{I}$ were achieved after $^{127}\text{IOH}_2^+$ correction. Moreover, correction of mass-discrimination effects was done using an isotopic certified tellurium solution using $^{120}\text{Te}^{16}\text{O}/^{126}\text{Te}^{16}\text{O}$ on mass-shift mode.

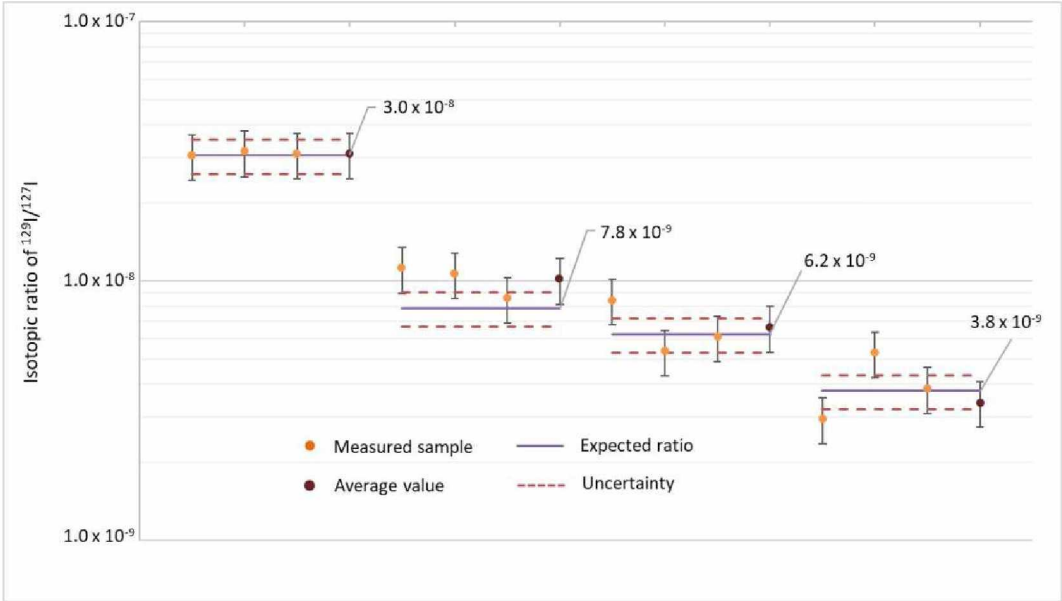


Figure 11 - Isotopic ratio $^{129}\text{I}/^{127}\text{I}$ determination in ICP-MS/MS on mass-shift mode in OM.

According to the fig. 11, the measured $^{129}\text{I}/^{127}\text{I}$ ratios were consistent with the theoretical values within the analytical error. Under this condition, the minimal $^{129}\text{I}/^{127}\text{I}$ was determined at 3.8×10^{-9} , an isotopic ratio never reached before¹⁵

Conclusion

In this study, ICP-MS measurement medium of iodine was studied and adapted to iodine's volatility. The memory and matrix effects were then minimized and the sensitivity was improved by a factor greater than 2. For the first time, ^{129}I is measured in mass-shift mode which allows a more consistent quantification by removing $^{129}\text{Xe}^+$ interference efficiently.

Moreover, the polyatomic interferences were also completely suppressed.

The ^{129}I quantification was based on the isotopic dilution technique using ^{127}I as internal standard. The previous determination of ^{127}I concentration is based on external calibration corrected with ^{126}Te as internal standard.

This new developed quantification method allows reaching ^{129}I limit of detection of 11 mBq L⁻¹. This detection limit is 10 times lower than the published one with ICP-MS/MS on on-mass measurement mode with O₂. Moreover, since only 15% of ^{127}I on mass-shift mode are detected, concentration that can be measured before the detector saturation are higher than on on-mass mode. Consequently, the reached $^{129}\text{I}/^{127}\text{I}$ with this new method is of 3.8×10^{-9} . This ratio is lower than that obtained on literature on on-mass mode.

Finally, this method was successfully applied to spiked environmental water samples.

Conflicts of interest

There are no conflicts to declare.

References

1. Kaiho, T. *Iodine chemistry and applications*. (John Wiley & Sons, Inc, 2014).
2. García-Torano, E. *et al.* The half-life of ^{129}I . *Applied Radiation and Isotopes* **140**, 157–162 (2018).
3. Frechou, C. & Calmet, D. Variations of iodine-129 activities in various seaweed collected on the French channel coast. *Czech J Phys* **53**, A83–A90 (2003).
4. Lefèvre, O. *et al.* Self-absorption correction factor applied to ^{129}I measurement by direct gamma-X spectrometry for *Fucus serratus* samples. *Nuclear Instruments and Methods in Physics Research Section A: Accelerators, Spectrometers, Detectors and Associated Equipment* **506**, 173–185 (2003).
5. Maro, D., Hebert, D., Gandon, R. & Solier, L. Dosage par spectrométrie gamma de l'iode 129 dans les échantillons biologiques marins et terrestres Application à des algues prélevées le long des côtes de la Manche : *fucus serratus* et *laminaria digitata*. *Radioprotection* **34**, 13–24 (1999).
6. Hou, X. Application of ^{129}I as an environmental tracer. *Journal of Radioanalytical and Nuclear Chemistry* **262**, 67–75 (2004).
7. Hou, X. *et al.* A review on speciation of iodine-129 in the environmental and biological samples. *Analytica Chimica Acta* **632**, 181–196 (2009).
8. Fan, Y., Hou, X. & Zhou, W. Progress on ^{129}I analysis and its application in environmental and geological researches. *Desalination* **321**, 32–46 (2013).
9. Arnold, M. *et al.* The French accelerator mass spectrometry facility ASTER after 4 years: Status and recent developments on ^{36}Cl and ^{129}I . *Nuclear Instruments and Methods in Physics Research Section B: Beam Interactions with Materials and Atoms* **294**, 24–28 (2013).
10. Ruge, G. *et al.* The first four years of the AMS-facility DREAMS: Status and developments for more accurate radionuclide data. *Nuclear Instruments and Methods in Physics Research Section B: Beam Interactions with Materials and Atoms* **370**, 94–100 (2016).
11. Jacobsen, G. E. *et al.* AMS measurement of ^{129}I , ^{36}Cl and ^{14}C in underground waters from Mururoa and Fangataufa atolls. *Nuclear Instruments and Methods in Physics Research Section B: Beam Interactions with Materials and Atoms* **172**, 666–671 (2000).
12. Hou, X. & Hou, Y. Analysis of ^{129}I and its application as environmental tracer. *J. Anal. Sci. Technol.* **3**, 135–153 (2012).
13. Kutschera, W. AMS Facilities of the World. (2012).
14. Warwick, P. E., Russell, B. C., Croudace, I. W. & Zacharauskas, Ž. Evaluation of inductively coupled plasma tandem mass spectrometry for radionuclide assay in nuclear waste characterisation. *Journal of Analytical Atomic Spectrometry* **34**, 1810–1821 (2019).
15. Díez-Fernández, S., Isnard, H., Nonell, A., Bresson, C. & Chartier, F. Radionuclide analysis using collision–reaction cell ICP-MS technology: a review. *Journal of Analytical Atomic Spectrometry* (2020) doi:10.1039/DOJA00211A.
16. Flores, E. M. M., Mello, P. A., Krzyzaniak, S. R., Cauduro, V. H. & Picoloto, R. S. Challenges and trends for halogen determination by inductively coupled plasma mass spectrometry: A review. *Rapid Communications in Mass Spectrometry* **34**, e8727 (2020).
17. Isnard, H., Nonell, A., Marie, M. & Chartier, F. Accurate measurements of ^{129}I concentration by isotope dilution using MC-ICPMS for half-life determination. *Radiochimica Acta* **104**, 131–139 (2016).
18. Ežerinskis, Ž. *et al.* Determination of ^{129}I in Arctic snow by a novel analytical approach using IC-ICP-SFMS. *Journal of Analytical Atomic Spectrometry* **29**, 1827–1834 (2014).
19. Yang, G., Tazoe, H. & Yamada, M. Improved approach for routine monitoring of ^{129}I activity and $^{129}\text{I}/^{127}\text{I}$ atom ratio in environmental samples using TMAH extraction and ICP-MS/MS. *Analytica Chimica Acta* **1008**, 66–73 (2018).
20. Ohno, T. *et al.* Determination of ultratrace ^{129}I in soil samples by Triple Quadrupole ICP-MS and its application to Fukushima soil samples. *Journal of Analytical Atomic Spectrometry* **28**, 1283 (2013).
21. Jones, S. D., Spencer, C. P. & Truesdale, V. W. Determination of total iodine and iodate-iodine in natural freshwater. *Analyst* **107**, 1417–1424 (1982).
22. Farcet, J.-B., Kindermann, J., Karbiener, M. & Kreil, T. R. Development of a Triton X-100 replacement for effective virus inactivation in biotechnology processes. *Engineering Reports* **1**, e12078 (2019).
23. Holubová, Z., Moos, M. & Sommer, L. Simultaneous determination of metal traces by ICP-MS in environmental waters using SPE preconcentration on different polymeric sorbents. *Chemical Papers* **66**, (2012).
24. Johnson, M. Detergents: Triton X-100, Tween-20, and More. *Materials and Methods* (2021).
25. Groot, M. T. D. & Merkx, D. M. *Electrochemistry of Immobilized Hemes and Heme Proteins PROEFSCHRIFT*.
26. Jiang, C., Brik, M. G., Srivastava, A. M., Li, L. & Peng, M. Significantly conquering moisture-induced luminescence quenching of red line-emitting phosphor $\text{Rb}_2\text{SnF}_6:\text{Mn}^{4+}$ through $\text{H}_2\text{C}_2\text{O}_4$ triggered particle surface reduction for blue converted warm white light-emitting diodes. *J. Mater. Chem. C* **7**, 247–255 (2019).
27. Oviedo, O. A., Reinaudi, L., Garcia, S. & Leiva, E. P. M. *Underpotential Deposition: From Fundamentals and Theory to Applications at the Nanoscale*. (Springer, 2015).
28. Shimada, A., Sakatani, K., Kameo, Y. & Takahashi, K. Determination of ^{129}I in the accumulated radioactive water and processed water of the Fukushima Daiichi Nuclear Power Plant. *J. Radioanal. Nucl. Chem.* **303**, 1137–1140 (2015).
29. Fujiwara, H., Kawabata, K., Suzuki, J. & Shikino, O. Determination of ^{129}I in soil samples by DRC-ICP-MS. *Journal of Analytical Atomic Spectrometry* **26**, 2528–2533 (2011).
30. Tanner, S. D., Baranov, V. I. & Bandura, D. R. Reaction cells and collision cells for ICP-MS: a tutorial review. *Spectrochimica Acta Part B: Atomic Spectroscopy* **57**, 1361–1452 (2002).

31. Jensen, B. P., Gammelgaard, B., Hansen, S. H. & Andersen, J. V. Comparison of direct injection nebulizer and desolvating microconcentric nebulizer for analysis of chlorine-, bromine- and iodine-containing compounds by reversed phase HPLC with ICP-MS detection. *Journal of Analytical Atomic Spectrometry* **18**, 891 (2003).
32. Bandura, D. R., Baranov, V. I. & Tanner, S. D. Inductively coupled plasma mass spectrometer with axial field in a quadrupole reaction cell. *J. Am. Soc. Spectrom.* **13**, 1176–1185 (2002).
33. Marie, V. Etude de la réponse des métallothionéines chez les bivalves, *Corbicula fluminea*, *Dreissena polymorpha* et *Crassostrea gigas*, après exposition au cadmium et au zinc : approches in situ et expérimentales. (Bordeaux 1, 2005).
34. Humans, I. W. G. on the E. of C. R. to. *Indium Phosphide. Cobalt in Hard Metals and Cobalt Sulfate, Gallium Arsenide, Indium Phosphide and Vanadium Pentoxide* (International Agency for Research on Cancer, 2006).
35. Alloway, B. J., Jackson, A. P. & Morgan, H. The accumulation of cadmium by vegetables grown on soils contaminated from a variety of sources. *Science of The Total Environment* **91**, 223–236 (1990).
36. Zheng, J. *et al.* Rapid determination of total iodine in Japanese coastal seawater using SF-ICP-MS. *Microchemical Journal* **100**, 42–47 (2012).
37. He, T. *et al.* A Rapid Acid Digestion Technique for the Simultaneous Determination of Bromine and Iodine in Fifty-Three Chinese Soils and Sediments by ICP-MS. *Geostandards and Geoanalytical Research* **42**, 309–318 (2018).